3 Biotech (2022) 12:299
https://doi.org/10.1007/s13205-022-03368-z

ORIGINAL ARTICLE

Gold nanogap impedimetric biosensor for precise and selective *Ganoderma boninense* detection

Thikra S. Dhahi[1,2] · Tijjani Adam[2,4] · Subash C. B. Gopinath[3,4,5] · U. Hashim[4]

Received: 27 April 2022 / Accepted: 17 September 2022 / Published online: 29 September 2022

Abstract

Ganoderma species are common wood-rotting fungi that cause root and stem rot in most monocots, dicots, and gymnosperms. It influences plantation crops such as oil palm and rubber in Malaysia, but the effects vary greatly within the genus. Because of the complex chemistry of Ganoderma, extracting and identifying the physiologically active chemicals is often time-consuming and necessitates extensive bioassays. This study investigated the specific identification of the most infectious Ganoderma species using a sub-20-nm gold electrode. Three electrodes were created using chemically controlled etching (2, 10, and 20 nm). An AutoCAD mask containing nanogap pad electrodes was used to create a chrome glass surface, which was then translated and built. Following the successful construction of the device, the sensor was evaluated using a combination of conventional photolithography and a size reduction technique to imprint the nanogap design onto the gold surface. *Ganoderma boninense* target DNA was synthesised and surface-modified to enable interaction at extremely low molecular concentrations. The proposed device has a detection limit of 0.001 mol/L, which is seven times lower than the detection limits of currently available devices. The capacitance, conductivity, and permittivity of complementary, non-complementary, single mismatched, and targeted biomolecules changed during hybridization. This sensor correctly differentiated between all samples. The sensor's performance is further validated by comparing experimental data from the sensor to theoretical data from the sensor's corresponding circuit model. The two data sets are very similar.

Keywords Electrochemical nanogap · *Ganoderma boninense* · Gold nanoparticles · Dielectrode

Introduction

The diseases basal stem rot (BSR) and upper stem rot (USR) caused by plant pathogenic fungus species (*Ganoderma boninense*) are the major source of economic losses in Malaysia and other Southeast Asian countries' oil palm industries. The fungus typically infects seedlings 1–2 years after planting and increases in crops 4–5 years old (Noor Azmi et al. 2020a, b). The disease that results on infected palms is significantly reduced the number of fresh fruit bunches produced determines the yearly harvest. Extensive research has been carried out over the last few decades to detect and control *G. boninense*, particularly during early growth and its aggressive pathogenicity, which has an impact (Ahmadi et al. 2017b). Despite this, there is currently no effective method for halting the disease's spread (Ahmadi et al. 2017a). Studies on early detection at the molecular level using electrochemical transduction are also scarce, particularly in Malaysia. The gravity of the situation necessitates the use of biosensors capable of detecting early disease. Small nanogap devices with tightly confined electrodes will have distinct advantages for nanobiosensing (Salazar et al. 2020). Electric field confinement can be greatly improved by reducing electrode dimensionality, increasing sensitivity and selectivity (Siddiqui et al. 2021). A smaller gap size

✉ Tijjani Adam
tijjani@unimap.edu.my

1 Electronics Technical Department, Southern Technical University, Basra, Iraq

2 Faculty of Electronic Engineering & Technology, Universiti Malaysia Perlis, 02600 Arau, Perlis, Malaysia

3 Faculty of Chemical Engineering & Technology, Universiti Malaysia Perlis, 02600 Arau, Perlis, Malaysia

4 Institute of Nano Electronic Engineering, Universiti Malaysia Perlis, 01000 Kangar, Perlis, Malaysia

5 Centre of Excellence for Nanobiotechnology and Nanomedicine (CoExNano), Faculty of Applied Sciences, AIMST University, Semeling, 08100 Kedah, Malaysia

improves screening and electrostatic tunability, allowing for faster detection (Noor Azmi et al. 2020a, b). The concept of electrochemistry is an interesting new feature of the nanogap, which can be used in many potential applications as the world faces serious new challenges. The study in this device will pave the way for more amazing applications by developing a device with an extremely small size (Salazar et al. 2020). The most fascinating and amazing effect is brought about by the gap as they get closer to each other. As the two sizes get closer together, they nearly overlap, resulting in a large electric field that is uniformly distributed throughout the entire electrode gap. The field created because of this phenomenon will significantly improve both the device's surface chemistry and electrical properties by introducing ion migration inside and outside the device, increasing the overall reaction rate and thus increasing device sensitivity and selectivity by reducing or eliminating screen time and false responses (Namhil et al. 2020). The application of such a device takes advantage of the dielectric and conductor interface mechanisms; when the analyte is brought closer to the device, it will respond to it (Husin et al. 2020). As the surface interact with the foreign materials, the surface charge across the gap induces electron excitation (Cho et al. 2022). The electron excitation is caused by the double-layer phenomenon of gap electrochemistry (Liu et al. 2020). In gold gap device, unique properties are introduced by taking advantage of the electrochemistry's strong surface chemistry due the gold high conductivity. Because of the rapid surface phenomena, the gap exhibits various impedance and dielectric properties that could have various applications and potential in biosensing, chemical sensing for ultra-sensitive sensing, and selective sensing (Kang et al. 2021). The device could be surface modified and used for an interesting application. Because of this adaptability, work on this device is being done with new structures and materials to investigate various effects and applications (Luo et al. 2020). Although the device has enormous potential, it is marred by several flaws, particularly the fabrication process (Pantazi et al. 2017). The fabrication of this device is extremely costly due to the use of expensive equipment (Perez et al. 2020). As a result, it is critical to implement techniques that could eliminate some processes and equipment to reduce costs and process time (Kumawat et al. 2019a; Kumawat and Pathak 2019). One of the most important solutions is to combine fabrication with chemically creating gaps with a controlled chemical process, which allows for the fabrication of nanostructures with extremely small features (Kumawat and Pathak 2021). On the other hand, the pathogenic fungus *G. boninense* continues to cause basal stem rot and upper stem rot diseases in the palm oil industry. Despite ongoing research, resolution is hampered by a lack of specific and sensitive devices to detect this fungus at an early stage (Oh et al. 2012; Shawky et al. 2018; Tamari et al. 2013; Lim et al. 2022). In this study, we created an extremely small size gap for detecting Ganoderma species using the specific and sensitive detection of *G. boninense*.

Materials and methods

Materials, nanogap fabrication and characterizations

The materials involved in the study are the silicon substrate, titanium rod, gold rod, photo resist, hydrochloric acid (HCl), ammonia hydrogen nitrate (NH_3), resist developer, 3-aminopropyl triethoxysilane (APTES), deionized (Di) water and synthesis sample group into probe, target, target complementary, target mismatch. The fabrication of nanogap is done, and the thickness, dimension and gap size were characterised morphologically and equally characterised electrically by measuring the capacitance, permittivity, conductivity, and resistivity curves using dielectric analyzer (DA). The gold gap was fabricated and characterise the nanogap structure before and after detection processes. Initially, 150 nm gold sheet was deposited on a silicon substrate prior this titanium of 50 nm was deposited on the silicon surface to increase adhesion between the gold and silicon substrate. To create gap, a resist was applied with coaster at 5000 rpm and at step of 100 rpm. This resist is dried for 30 min, exposed in UV light with the help of mask aligner for 30 s and developed for 30 s in a resist developer (Choi et al. 2019). This created an extremely small part of gap, and the gold layers was wet-etched using modified with Aqua-Regia (HCl 3:1 HNO_3) etched solution, the modification to optimise the re-action through DI water and mechanical agitation, all the processes of gap fabrication were done in class 1000 particles clean room at Universiti Malaysia Peris faculty of electronics engineering technology (FTKEN) under controlled humidity of 35–40% at below 20 °C. Upon completion of the fabrication, surface examinations were conducted to understand surface integrity, size, and nature of the gap, these were done using field emission scanning electron microscope (FESEM). Further, the materials were tested to confirm the existence of the intended materials. Upon confirming the materials and gap size, electrical measurement was conducted to identify the capacitance, permittivity, and conditions as various in the parameters are extremely in understanding the behaviour of the entire device. This was following the further electrical measurement upon the detection process, the device behaviour was monitored from the surface modification, probe, target, target complementary, target mismatch. The variations of the current, capacitance and permittivity were recorded discussed based on physical observation, academic observation and critical observation and comparison were made in the current state of the art and achievement in the

most literature. Moreover, to prevent nonspecific radicals' intervention, we coated the nonspecific area with glutathione because glutathione can block reactive oxygen species and other free radicals, similar claimed was reported by Zhao et al. (2021). Highlighting novelty of this work, to fabricate gold nanogap it is very important to control size and sharp of the gap produce due gold having large grain sizes where its depends on the accurate control of etching rate and chemical concentration. Herein, proposed novel and highly sensitive nanogap sensor is constructed using single step photolithography coupled with chemical etch. Well uniform Aunanogap was created in very 3 simple steps. This method is simple and fast, which provides a new path for fabricating large grain materials devices.

Boninense sample preparation and nanogap surface modification

The pathogenic fungus isolate *G. boninense* was collected from a field sample collection of diseased oil palm trees by the Malaysian palm oil board (MPOB) and was utilised as the target sample for DNA extraction analysis. *G. boninense* ssDNA was synthesised. The method for isolating genomic DNA from gram-negative bacteria was used to extract. A 1.5 mL micro centrifuge tube containing 1 mL of overnight grown bacteria was spun at 16,000 revolutions per minute for 2 min at 5 °C using an Eppendorf centrifuge 5430 (Germany). After discarding the supernatant, 600 L of lyse buffer was progressively added to the bacterial pellet until it became suspended as proposed (Hamdy et al. 2018). To lyse the cell walls, the pellets were incubated for 5 min at 80 °C in a water bath (Stuart water bath, UK) before being cooled to room temperature. Three litres of RNase solution was added to the cell lysates and mixed inverted. After incubation at 37 °C for 15–60 min, the samples were cooled to room temperature. To precipitate the proteins, 200 mL of protein precipitation solution was added to the RNase-treated cells. After mixing for 20 s with a maximum speed vortex (LMS, Japan), the solution was incubated on ice for 5 min before being centrifuged at 16,000 rpm for 3 min. The DNA supernatant was transferred to a new 1.5 mL micro-centrifuge tube containing isopropanol and gently inverted until thread-like strands of DNA formed and condensed into a visible mass based on the protocol provided by Oh et al. (2012). The tubes were centrifuged at 16,000 rpm for 2 min, and the supernatant was discarded carefully. The pellet was discharged onto cleaned absorbent paper. The DNA pellet was washed with 600 L of 70% ethanol, gently inverted several times, and then centrifuged for 2 min at 16,000 rpm. Aspirating the ethanol gently, emptying it onto clean absorbent paper, and allowing it to air-dry for 10–15 min (Uda et al. 2021). The cells were treated with 100 mL of the DNA rehydration solution and incubated at 65 °C for 1 h before the DNA pellet was rehydrated at room temperature overnight. After that, the modified nanogap surfaces were incubated for 5 h at 25 °C with 0.5 L of 10 nmol/L probe DNA. A phosphate buffer saline (PBS) wash and moderate nitrogen flow were used to dry the unbound probe three times (Tamari et al. 2013). Finally, the probe-attached nanogap surfaces were incubated for 4 h at 25 C with 0.5 L of complementary, non-complementary, and single mismatched DNA targets at 10 nmol/L. Before being dried with a moderate nitrogen flow, the unbound targets were washed three times with a 10 nmol/L PBS buffer. This section describes a straightforward technique for detecting DNA through immobilisation and hybridization. To modify the surfaces of the gaps, the DNA-amine group was selected. DNA-amine was used as an adhesive to mark APTES and link probe-DNA strands. Prior to probing DNA immobilisation, the nanogap surfaces were cleaned with DI water, modified with DNA-amine (10 nmol/L DNA-amine was dropped on the electrode surface for a whole night before washing with DI water and drying at room temperature), and tagged with gold nanoparticles (AuNPs) and, to prevent nonspecific radical intervention, glutathione. Glutathione is capable of preventing damage to important cellular components caused by reactive oxygen species and other free radicals. The thiol-probe DNA, complementary, non-complementary, and single-mismatched targets are prepared. Prior to immobilising the probe DNA, the nanogap electrodes were heated to 60 C and 0.5 L of 10 nmol/L APPTES was poured into the gaps and incubated for 10 min to dry them. The particles that were just loosely adhered were gently washed with DI water and dried under a moderate nitrogen flow. The whole procedure was repeated to increase the concentration of APTES on the nanogap surfaces. Detections were monitored based on electrical tests for DNA detection utilising nanogap electrodes. These were performed using a dielectric analyzer, Novocontrol technologies, handsangen, Germany) with a base voltage of 1.0 V. Capacitance, conductivity, and permittivity profiles were determined for nanogap electrodes that were left unaltered, modified, probe immobilised, and target hybridised (Adam et al. 2021a).

Results and discussion

Bare nanogap sensor surface morphology and electrical characterizations

This section presents the result surface morphology and electrical characterisation of the bare device where the gap produced through the chemical etching gaps were determined using a field emission scanning electron microscope (FESEM). This development in the nanogap, and a minimum nanogap size of 5 nm was achieved, as can be seen

in the FESEM observation. It is worth noting that etching is crucial in achieving the smallest possible gap size. 2 nm was reached with three cycles of wet etching on the initial marked gap structure using aqua regia solution with time control. When the etching time is increased from 6 to 9 min, the etching rate increases as well. The etching of gold requires a controlled method since the substance has a very high density, estimated to be 19.3 g/cm^3, which enables the gold to have extremely strong atomic bonding and lager grain size as shown in Figs. 1 and 2. It has a cubic

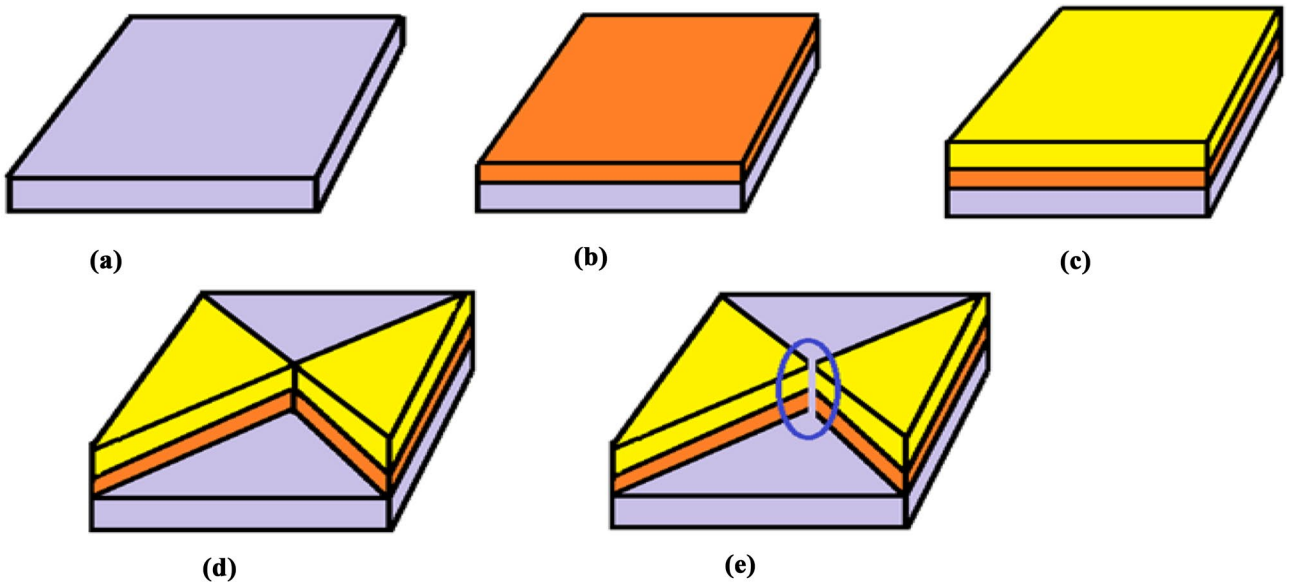

Fig. 1 Nanogap **a** substrate, **b** device material deposited, **c** photoresist coated, **d** development and exposure, **e** etching

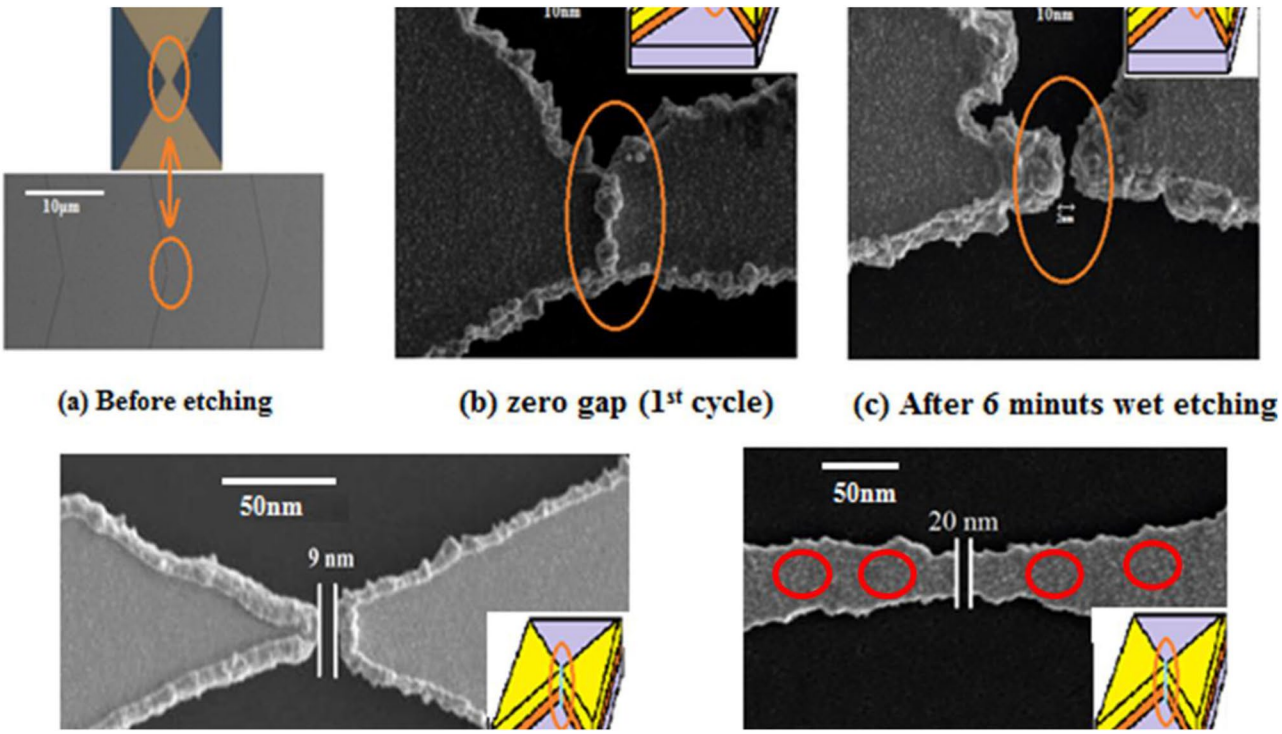

Fig. 2 Etching process to achieve smallest nanogap

face-centred crystal structure with an extremely high atomic pack density, which qualifies gold as a noble metal. It has the best oxidation resistance because it occupies the 5d orbital, which is fully outside the single valence electron and therefore highly protected from any reaction partners. As a result, the wet reaction etching of gold necessitates the use of a powerful oxidant to cope with the unpaired valence electron. However, owing to the broad grain boundary of the wet etching still preparation, production using traditional lithography may be more cost effective and advantageous. Aqua regia is a chemical composition that is frequently used to etch gold. It is a combination of hydrochloric acid and nitric acid. Depending on the concentration, the combinations may etch gold at room temperature in a relatively short period of time. The combination has a significant oxidative impact because, after combining hydrochloric and centric acid, a radical component known as nitrosyl chloride (NOCL) is produced, as indicated in the reactant side of Eq. (1). The chemical process during etching is as follows, with the presence of radicals as well as free Cl radicals in the solution maintained throughout the reaction where the noble metal dissolves as Cl-complex compound is produced (tetrachloride gold-(III)-acid = $HAuCl_4$). The reaction between HNO_3/HCl mixes is unstable and decomposes with the production of nitrogen oxides and Cl_2 gas; therefore, the disintegrated material etches away. The etching rate of the procedure is adjustable, and the rate of aqua regia for gold is set at about 10 m/min at room temperature. This rate may be decreased or raised based on the concentration of the mixture, temperature, and in the case of this research, it has exceeded 10 nm/min. where the device etch depth at the resolution of 5 nm/min was found with uniform ratio after 5 successful fabrication processes repeated (Shukla et al. 2017). The etch rate was controlled by the temperature. It was found that at 60 °C a constant and uniform etching was obtained. After 1 min 0.1 µm and 5 nm axial depth and radial were obtained respectively. This was reported 5 times in order confirmed the repeatability of this process:

$$HNO_3 + 3HCl \rightarrow NOCl + 2Cl + 2H_2O. \quad (1)$$

Overall smallest gap of 9 nm was realised generated gaps between Au/Ti electrodes ranging from 9 to 20 nm depending on the duration for the wet-etching procedure. The schematic, however, indicates an increase in the size of the gap with etching time, as shown in both images. The gap varies from 50 to 10 nm when the etch time is increased from 6 to 15 min reached 5 nm. It is easy to adjust the gap size from the etching formulation by altering a single or two etching factors such as concentration and etch duration. However, the main important parameter is the temperature. It is also essential to draw to the reader's attention that. Other factors, such as temperature, also played a significant part in encouraging the etch, and it has been claimed that the etch may rise by a factor of ten with temperature. Before proceeding with the electrical characterization procedure, physical characterization was conducted. The most significant parameter is the gap where it plays and important role in the entire performance of the sensor. Therefore, the nature of the nanogap was determined through doing analyses where three independent analyses were conducted to verify this. The FESEM morphology, XRD, and FTIR analysis are depicted in Figs. 2, 3a, b, respectively. The FESEM imaging was conducted to determine the morphological properties of the nanogap materials. These findings demonstrate that the observed morphology is shallow like shape. This gap distribution was estimated, and the results were found to be consistent with the XRD data where the gap size is between 1 and 20 nm based on the scale. Figure 3b displays the XRD pattern of the gold (b) crystal planes (101), (100), (111), (101), (131), and (011) are depicted by peaks at 2 = 34.0043°, 34.8021°, 37.0442°, 49.0084°, 59.1117°, 64.3313°, and 69.5005°, respectively. Moreover, the gap was measured for I–V characterisation using an electrical probe, and the procedure was carried out in a vacuum chamber. It has been discovered that current rises with voltage, particularly at voltages greater than 6 mV. Figure 4 depicts the capacitive, permittivity and conductivity of the constructed nanogap structure prior surface modification. The is the typical characteristics of bare nanogap and in fact, the gap I–V characteristics of a typical planar gap device and it shows a transition state from the Fowler–Northeim diode relation Child–Langmuir law The significance of the fabrication is emphasised. It verified the existence of space charge effects with the presence of gap voltage and gap spacing. nanogap electrochemical sensors have demonstrated their superiority among many methods used in detecting the presence of biomolecular species in various forms, including free and chemically conjugated variants, by distinguishing the changes caused by modifications introduced into the polar properties of these molecular species and their response to an electric field applied across the electrodes, in addition to the changes introduced in the double-layer formation. Particularly, molecular species with diameters in the range of a few nanometers have a strong effect on the electrochemical conditions across a nanogap, resulting in enhanced detection without the need of labelling as in other methods. The geometrical design of the gap determines the relative degree of impact of these two conditions, ionic characteristics and double-layer development, as stated before. The optimization of the gold materials and planer geometrical design for the produced nanogap device, on the other hand, will confuse these two conditions[1]. Furthermore, in the case of planar nanogaps, employing any kind of FESEM imaging is useful for determining the existence of molecular species as well as detecting electrochemical changes based on either admittance

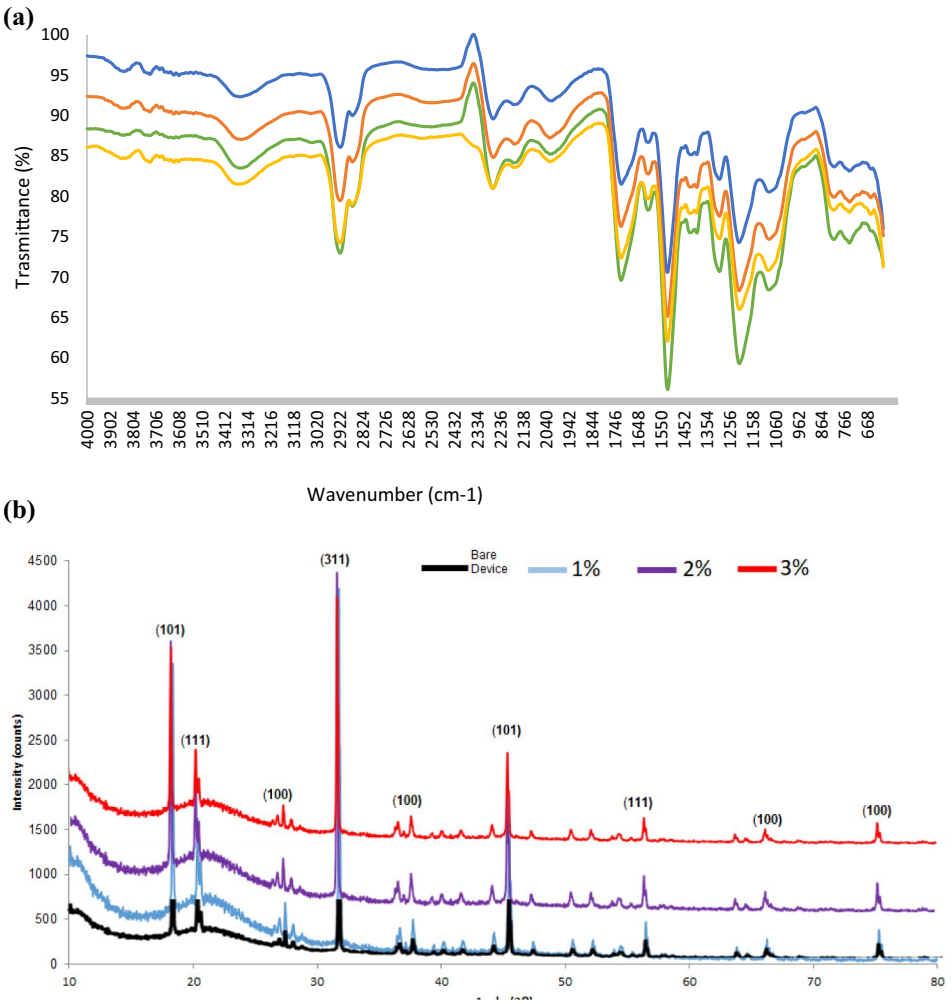

Fig. 3 **a** FTIR spectra of the nanogap, **b** XRD spectra of the nanogap

or conductance changes, as the case may be. In this situation, planar type nanogaps are more flexible in terms of detection when compared to other geometrical designs. The success of a planner nanogap sensor in a biosensor application is ultimately determined by the following criteria. Ease of manufacturing, flexibility in creating various inter-electrode gaps, electrode material compatibility with the molecular species under consideration, reuse of sensing components by simply removing the electrolyte in the previous measurement greater sensitivity, and ultimately cost more. The superiority of the technique based on CMOS processing using standard IC procedures is shown by the various ways utilised to manufacture nanogap structures. The use of gold electrodes is beneficial in many instances, such as improved affinity to DNA strands through thiol radical attachment, as will be verified in future research. In the instance of a metal–oxide–semiconductor structure, the capacitance was permittivity were and conductivity were measured. To demonstrate the effect of high and low frequency response principles with various gap sizes of 3-, 9-, and 20-nm gold nanogap structures, the applied voltage at the metal electrode, on the other hand, will be affected by the band structure of the metal electrodes since the carriers are one kind on which the electric field terminates. Under these circumstances, the valance band of a MOS capacitor is closer to the conduction band, and electrons are readily given or accepted to pass across the conduction region. Furthermore, as shown in Fig. 3, the capacitance variation of this structure increases with the regimen gapes for the produced nanogap, similar result is presented in various studies, among them Khaliq et al. (2021).

Characterization of surface modified and biomolecular detection of nanogap biosensor through capacitive and permittivity changes

The primary aim of biosensors is to achieve high performance with enhanced sensitivity, selectivity, reliability, and reproducibility, as well as dependability and reproducibility (Adam and Hashim 2015). Researchers have been working on the creation of portable bio-sensing handheld devices that may provide the appealing characteristics while remaining as inexpensive as feasible. Diagnostics based on molecular

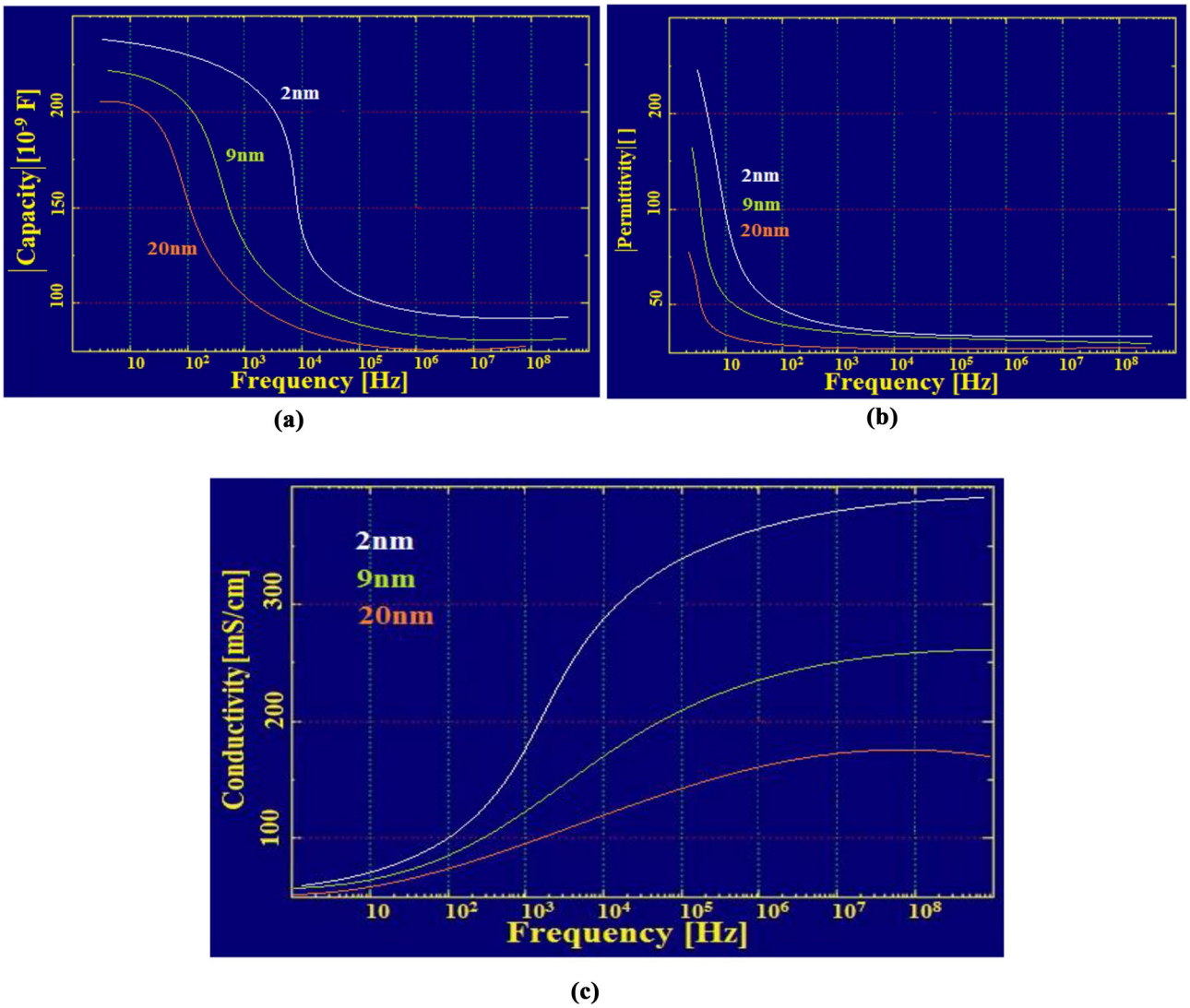

Fig. 4 Electrical characterization of the bare device **a** capacitive behaviour of the gap, **b** permittivity of the gap, **c** conductivity of the gap

detection are being included into new screening techniques, and they can identify infection or viral integration into the host cell. A new generation of nanotechnology for device validation and clinical impedance screening based on nanobiosensors has been created to solve current issues and make it simpler for physicians to detect a specific illness and propose the most suitable treatment plan in less time. To assist in the creation of a united effort, we must emphasise nanotechnology as a critical component in attaining success in today's global scenario (Oh et al. 2012). It bridges the gap between the laboratory and industry by adapting existing laboratory settings to the new hand-held device using modified micro-/nanodevices. According to these possibilities, present research is being conducted with the primary aim of collecting essential information on nanomaterials to progress the development of nanobiosensors that will be helpful to all levels of stakeholders in the long term. The ability to distinguish between complementary and non-complementary targets, as well as single mismatch targets, is a need for the biosensor. The study goes into great depth on the device's unique feature. Several researchers have proposed methods for the electrical detection of biomolecules in their respective fields (Jiang et al. 2018). However, in their research, a gap greater than 100 nm was utilized to detect and hybridize a DNA-based biomolecule biosensor. This research aims to decrease the gap distance between two electrodes to less than 10 nm (nm) or less. It was decided to manufacture nanogap electrodes with a smaller gap size (5 nm) to minimize and perhaps eliminate the impact of parasitic capacitance. Modification of the surface by the amino group is accomplished via the use of APTES linked. Surface modifications are utilized to enhance sensitivity by bridging the two electrodes

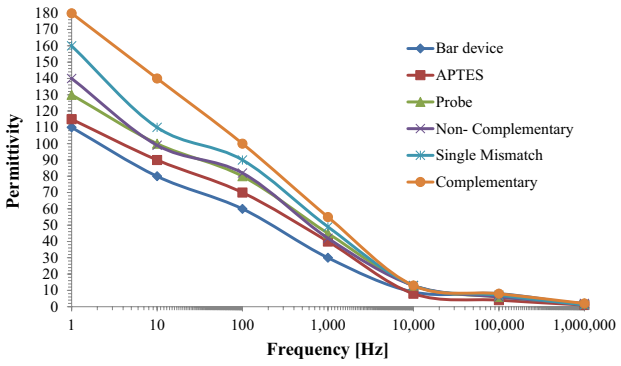

Fig. 5 Electrical characterization of the surface-modified nanogap biosensor showing variation of permittivity with the frequency in respect to different surface chemistry

in the nanogap structure, which leads to the formation of a connection between the Covid stranded between the nanogap and the facilitation of the flow of electrons via the electrical detection process. Changes in capacitance, conductivity, and permittivity were measured before and after probe-DNA immobilisation and various types of DNA hybridization (complement, non-complement, and single mismatch) as a function of frequency were detected. After hybridizing Figs. 5 and 6, the values of capacitance, and permittivity all indicate an increase in value. The conductivity profiles of the nanogap improved gradually with the addition of each layer of surface treatment. The results of combining the APTES, probe, and following target samples, which are classified as non-complementary, single mismatch, and complimentary. As previously mentioned, the increase in conductivities was most likely due to the gap narrowing effects of the nanogap gold, which happened because of these layers filling the gap upon deposition on the side wall and also onto the gap spaces. Moreover, the figure shows the change in electrical profiles for nanogaps, with significant variances in resistance due to frequency variations, suggesting intrinsic electron confinement Fig. 7.

Determination of the detection limit

The detection limit was determined with changes in conductivity and conductivity refers to a medium's capacity to respond to changes in electronic exchange and dipole reorientation because of a changing electric field. Due to the large gap time at low frequencies, there is an exceptionally high chance of reorienting the dipole. At higher frequencies, the mean interval length allows for polarity shifts and reorientation of the dipoles, which results in stronger signals. At high frequencies, however, the signal polarity changes too rapidly,

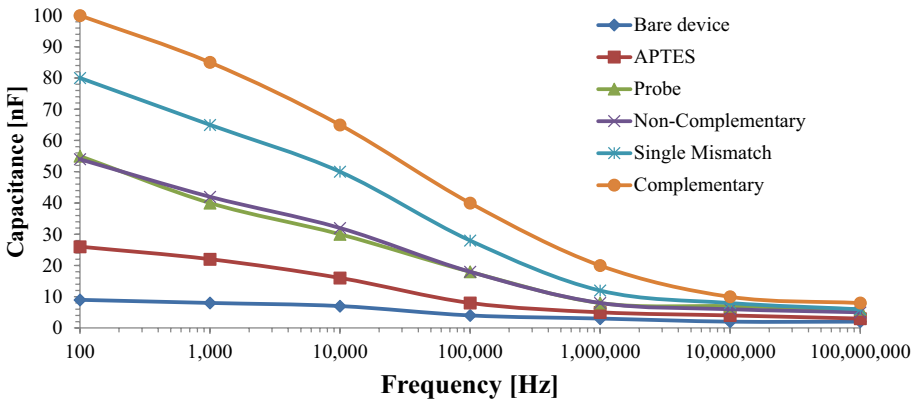

Fig. 6 Electrical characterization of the surface-modified nanogap biosensor showing variation of capacitance with the frequency in respect to different surface chemistry

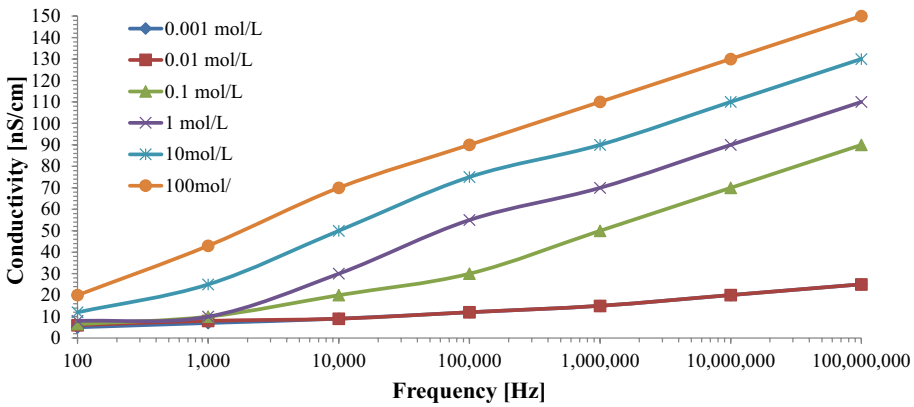

Fig. 7 Electrical characterization of the surface-modified nanogap biosensor showing variation of conductivity with the frequency in respect to concentration

leaving the dipoles with little time to reorient and respond to the changing field. Therefore, dipoles are too slow to respond to changing electric fields at high frequencies, making the medium insensitive to changes in permittivity. In the other hand, the initial response of the sensor was determined through the nanosensor response to the target sample (complementary sample) concentrations of 0.00, 0.01, 0.1, 1, 10 and 100 mol/L with tenfold serial dilution were monitored to obtained limit detection of detection. Although, the sensor shown excellent speciality to prevent nonspecific radicals' intervention, we coated the nonspecific area with glutathione because glutathione can block reactive oxygen species and other free radicals. For the purpose comparative, all samples were detection under same conditions and concentration. Currently available literature does not contain any information on how to modify the sample concentration of electrodes with nanogaps. On the other hand, some studies have reported on an optimization study for bacteria concentration on nanogap using antibody immobilisation as a method of optimization. In their tests, they discovered that the detection limit was reached at an optimal concentration of 6.73 CFU/mL. In the current study, it was found that the optimal concentration was 1 mol/mL of the compound. This concentration was also 7 times lower than the concentration discovered in various studies, which was another positive finding. Each concentration of sample is obtained for 0.001, 0.01, 0.1, 1, 10 and 100 mol/L with tenfold serial dilution as shown in Fig. 8.

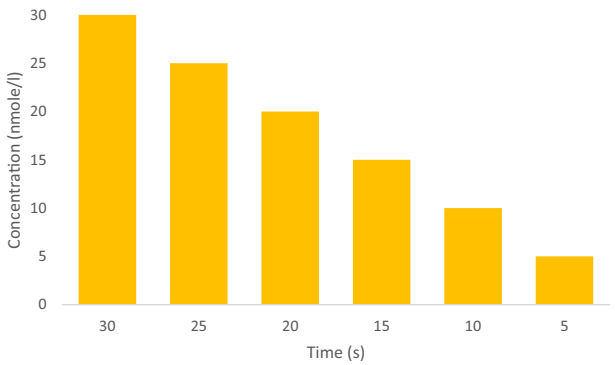

Fig. 8 The response of the nanogap biosensor based on concentration and time

Linearity of the nanogap biosensor

For a series of measurements with varied analyte concentrations, linearity is defined as $y = mc$ where m is the biosensor's sensitivity and c is the analyte concentration. The linearity of a biosensor affects its resolution and the concentration range it can test. A biosensor's resolution is the smallest change in analyte concentration required to modify the biosensor's response. Depending on the application, a high resolution is required, since most biosensors need not only analyte detection but also concentration monitoring over a wide range. The linear range is the range of analyte concentrations for which the biosensor response fluctuates linearly with concentration; Fig. 9 shows the typical linear trend; this confirmed the sensor ability to any changes. A biosensor's limit of detection (LOD) or sensitivity refers to the smallest quantity of analyte that it can detect. A biosensor is needed in a variety of medical and environmental monitoring applications to detect analyte concentrations as low as ng/mL or even fg/mL to confirm the existence of traces of analytes in a sample. Nanogap biosensor based on electrode ga also known as double-layer bio-transducer, are known for their specificity towards the biomolecule, which can be explained

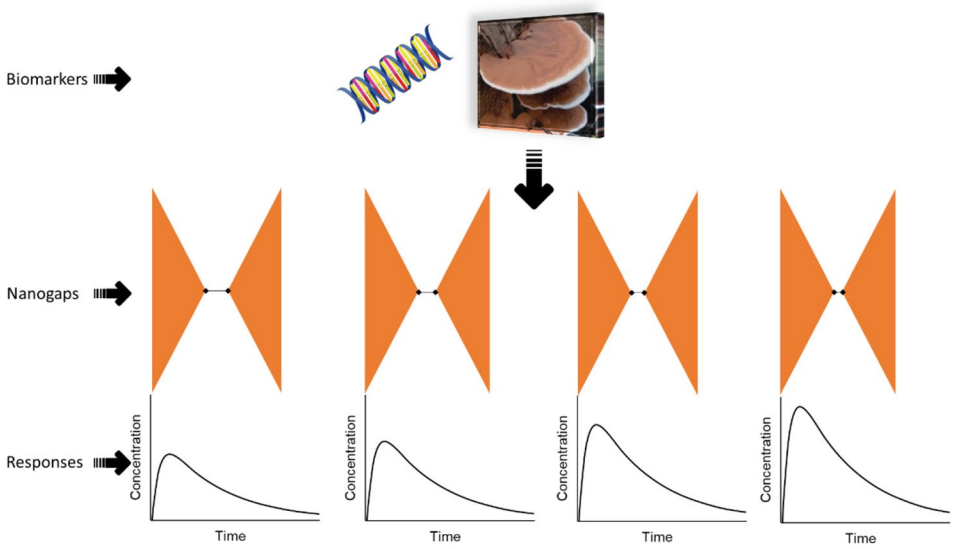

Fig. 9 Concept of surface modification, gap size and linear response

by impedance response induced fit model. The biosensors are bio-capacitive in nature. They convert the analyte ohmic to a impedance with the gap capacitive effect, which can be measured by the change in impedance parameters such as charge, capacitance and impedance shift. The biomolecule is placed close to the transducer surface or embedded in conducting nanomaterials for a faster and short diffusion path for enhanced signal generation and enhance surface chemistry. This work is a nanogap-based biosensing platform represents the organization of two conductive electrodes separated by no more than 20 nm. Gold nanogap were used for the detection of Ganoderma biomolecular which created interactions due surface chemistry introduce nanogap electrodes are important tools for the investigation of material properties at the manometer scale or at the molecular level. They might be considered as building blocks for the construction of nano-circuits and nanodevices, the illustration interactive mode of biosensor is shown in Fig. 10.

Nanogap biosensor theoretical data based on the sensor equivalent circuit simulated result

In order to establish the fundamental behaviour of the nanogap biosensor, it equivalent circuit was established based capacitors and resistors arrangement with the circuit designed, the biosensor structure was modelled with the equivalent circuits as shown in the above section. The sensor consists of two electrodes which are separated by a distance on the order of 2 nm, the field effect of electrical is eliminated in this design in the compact design. Thus, the entire nanogap biosensor was modelled with capacitance and resistance connected in parallel to imitate the typical nanogap. The parameters were measured with extracted value from the circuit simulation where impedance values using at different frequencies were obtained. It was found the impedance changes with respect to frequency were observed. Experimental was conducted with various frequencies of the applied signal were also observed for the five different biomolecule concentrations. Figure 11 shows the electrode electric field of the entire biosensor, it mechanism is as follows, the field exponentially with increasing in strength with distances reducing in other word when the gap reducing as illustrated. As shown the filed will field decays in a region determined by the size of the sensor gap. Thus, the electric filed of the nanogap is largely depends on Debye length (Oh et al. 2012). The sensor domain is act as electrolyte since the biomolecule is in solution and according to well established classical electrolyte theories interactions less concentrated ion domain, the field strength decay exponentially with distance. Thus, with gap distance characteristic length scale where the entire sensor depends on. The two electrode acts as a shield against the applied electric field. In some case, depending on materials, causes a major problem for the biosensor applications since the electric field applied by the electrodes does not appear on the significant portion of the target medium. The problem is solved with gold electrode due to the gold large gain size (Adam et al. 2021b). The large grain size of the gold increases the Debye length and decreasing the effect of the electrode separation distance. Moreover, to gain understanding inside device behaviour fundamentally, Electrochemical processes associated with the electrolyte/interface and redox reactions are simulated/computed as an electric circuit (equivalent circuit) involving resistors and capacitors where were representing the targeted element and device gap. This equivalent circuit is designed and implemented to understand and evaluate the individual components of the biosensor sensor system. In the engineering world, "Nyquist plots" are quite prevalent. The Nyquist plot is a logarithmic representation of the impedance of an electrical circuit. Another approach to visualise

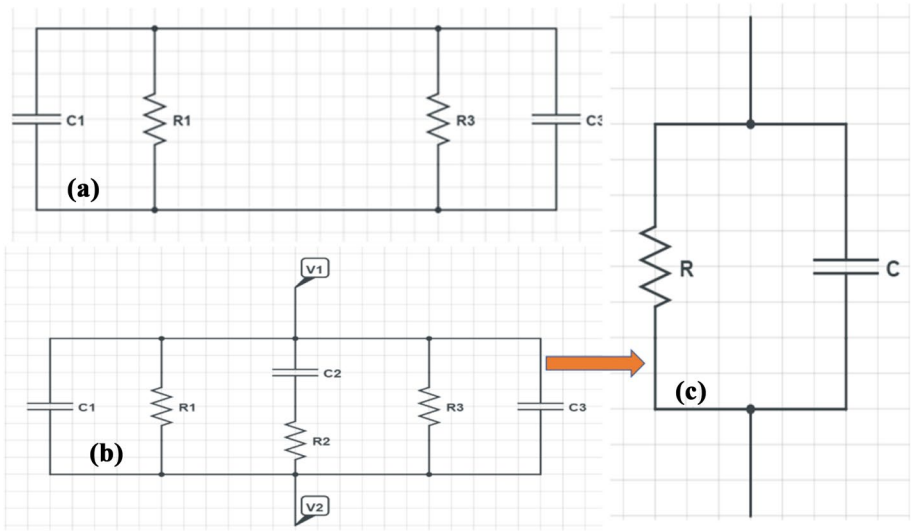

Fig. 10 Nanogap biosensor equivalent circuit

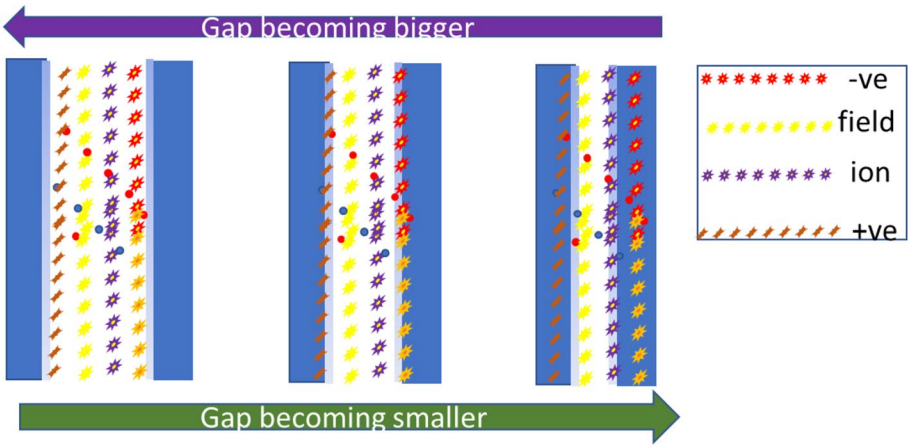

Fig. 11 Nanogap biosensor mechanism, illustrating the electric field strength between the two electrodes as size changes

the data is via a Bode plot, which plots the magnitude and impedance independently, furthermore, the figure presents the Nyquist plots of the impedance spectroscopic responses of our biosensor to different to the deference concentration of the Ganoderma molecule. The electron transfer resistances (the diameters of the semicircles at the *x*-axis) of the sensor increase with increasing cell concentration and the curve fit with the behaviour of equivalent simulated based on EIS software. In 1975, electrochemical impedance spectroscopy was invented. Impedance is determined by applying a potential wave and recording the current wave that results. EIS is classified into two types: Faradaic and non-Faradaic. The total impedance of a circuit may be calculated using Ohm's law. The Warburg impedance (W), which is frequency dependent, may be created by the diffusion of molecules or redox species. As the frequency rises, the distance that diffusing reactants must travel decreases, and the resistance increases as the redox molecules exert more effort to diffuse Lim et al. (2022).

Comparison of nanogap biosensor experimental data and theoretical data

To valid the response of the, a comparison was drawn between the theoretical and experimental data, the theoretical was obtained based on simulated result from the equivalent circuit. Figure 12 shows the fitting curve based on the real impedance shift and imaginary impedance for the two data. The impedance shift has confirmed the conductivity of the device as the surface is modified. If the gap is too small (2 nm), anything coming in between this gap render short circuit and making the sensor behave like a conductor. The changes in permittivity between the nanogap electrodes before and after the hybridization processes, which were performed at various frequencies and utilizing different states. The target and the probe are hybridized if the measurements reveal a significant variation in permittivity value between the target and the probe. Unless otherwise

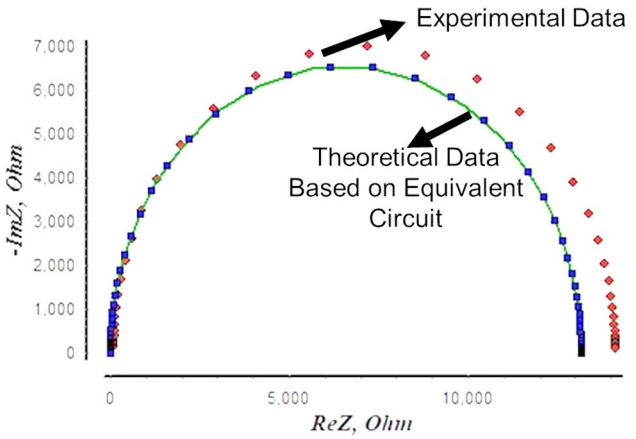

Fig. 12 Comparison of the theoretical and experimental data

stated, if no response is recorded in the measurement, it is deemed a mismatch or non-complementary. In the research of Khaliq et al. (2021), the results of nanogap electrodes before and after DNA hybridization using a variety of ionic strength electrolytes were compared to each other. In contrast, the permittivity measurements were increased after hybridized DNA was used for a short period of time, and then decreased at 200-Hz (for a short period of time). This was due to the solution between the larger size of the gap (> 20-nm) causing the solution to dry faster by providing enough space for the air to pass through the nanostructure. With rising frequency and various gap circumstances in the present experiment, the stability of permittivity profiles was found to be improved, and it then began to decline further at 1000 Hz, as the frequency was increased further (Kumawat and Pathak 2021). Comparing the capacitance measurements for the nanogap electrodes, it was discovered that the number of gold nanoparticles with 5-nm polysilicon was higher than in the literature nanogap devices, resulting in high capacitance and confirming once more the excellent performance for the nanogap electrodes in this study.

The nanogap electrodes in this study have low resistivity and good conductivity. The lower resistivity and higher conductivity of the devices may be wing to the greater mobility of the surface electrons, which may explain their lower resistivity and higher conductivity. An electrochemical biosensor is a device that may provide quantitative or semi-quantitative analytical data. The interaction of the target molecule with the detecting surface causes changes in current, potential, conductance, or field effect, which are measured by EC biosensors. Biosensors that monitor an electrochemical cell's potential at the working electrode. Potentiometry measures redox activity within EC cells. The Nernst Equation governs the relationship between potential and concentration as shown. Impedance changes can show the detection of various biomolecule such as antigen–antibody, biotin–avidin, oligonucleotide–DNA interactions. on electrode surfaces. Interdigitated microelectrodes are now being used in biosensors due to microfabrication advances. The sensor is a two-electrode configuration for electrical impedance measurements. The equivalent circuit for the IME device consists of an ohmic resistance of the electrolyte between two sets of electrodes and the double-layer capacitance, an electron transfer resistance around each set of electrodes. Synthetic 5′-amine-terminated single-stranded oligo"-nucleo"-tides were immobilized on the gold gap surface between the metallic digits of sensor electrodes. Non-specifically adsorbed probes onto the metallic electrode were removed by a 5 steps cleaning. The sensor provides a useful means to directly detect the hybridization of DNA strands. With clearly show different trend for the probe, complementary, non-complementary and the mismatch. The relative impudence versus. frequency curve for targeted biomolecule obtained using nanogap measurement sensor is very close to the theoretical value at low frequency is high, diminishes in high frequency for the impedance, this behaver is exactly opposite with impedance shift. Normal electrochemical cell interactions involve concentration of electroactive species, charge and mass transport from bulk solution to electrode surface. Use the Electrochemical Interactions Simulator to investigate these processes. Here we investigated the behaviour impedance with frequency increased. On a Nyquist plot, impedance can be represented as a vector (arrow) of length $|Z|$. Another way to express it is called a Bode plot, where magnitude vs. frequency and impedance are plotted. The Nyquist plot illustrates the system's resistance, which is equal to the sum of analyte resistance) and (charge transfer resistance). The relationship between double-layer capacitance, charge transfer resistance, and frequency can be used to define an electrochemical reaction's time constant. On a logarithmic scale, the Bode plot depicts the absolute impedance Z as well as the impedance shift as a function of frequency (Chiang et al. 2019). The impedance shift versus frequency plot is highly dependent on system characteristics and may be used to compare actual findings to the corresponding circuit model in theory. The Nyquist and Bode plots of system element behaviours for both Faradaic and non-Faradaic impedance sensors. It can be readily shown that the system is resistive at high and low frequencies due to the absence of impedance shift, but capacitive at intermediate frequencies due to the impedance shift.

Conclusion

The presented novel technique for fabricating nanogap devices with a 2 nm gap has been demonstrated to be used as a nanosensor in detecting plant disease. The gap I–V characteristics of a typical planar gap device are presented here, and the device exhibits a transformation state derived from the Fowler–Northeim diode relation and the Child–Langmuir law. The significance of the fabrication is emphasised in the text. It verified the existence of the space charge effects in the presence of the gap voltage and the gap spacing, which was previously suspected. Aside from that, a simple and repeatable electrical detection method based on *Ganoderma boninense* (*G. boninense*) detection and nanogap electrodes was proposed. For the first time, the nanogap structures were modified with the *G. boninense* probe-amine group to create an attachment site for the thiol-tagged probe. In addition to providing a surface for the attachment of probe DNA, the surface treatment substantially improved the sensitivity of the biosensor used. The created biosensor successfully identified complementary, non-complementary, and single mismatched DNA targets by measuring the changes in capacitance, conductivity, and permittivity of the nanogap electrodes as a result of the hybridization of the target DNA sequences. The nanogap structure, on the other hand, exhibits the same patterns in the increase of capacitance, conductivity, and permittivity with various situations of detecting step as has been seen in the literature. The detection limit for the proposed device is 1 mol/L, which is seven times lower than the current detection limit in the market. Furthermore, it is worth noting that the device's behaviour before and after detection is similar and identical. Thus, this has fully confirmed the ability of the device to discriminate various ions. However, there is still room for improvement by looking at the effect of interfering ions to measure the efficacy of prepared nanogap during the existence of other molecules, especially species of the targeted molecules. We recommend study toward this, and we are equally expanding toward this, which will be included in our next publication.

Declarations

Conflict of interest The authors declare that they have no conflict of interest in the publication.

References

Adam T, Hashim U (2015) Highly sensitive silicon nanowire biosensor with novel liquid gate control for detection of specific single-stranded DNA molecules. Biosens Bioelectron 67:656–661. https://doi.org/10.1016/j.bios.2014.10.005

Adam T, Thikra D, Gopinath S, Hashim U (2021a) Novel approaches in fabrication and integration of nanowire for micro/nano systems. Crit Rev Anal Chem 6(7):99–107. https://doi.org/10.1080/10408347.2021.1925523

Adam T, Dhahi TS, Gopinath SCB, Hashim U, Uda MNA (2021b) Recent advances in techniques for fabrication and characterization of nanogap biosensors: a review. Biotechnol Appl Biochem. https://doi.org/10.1002/bab.2212

Ahmadi P, Muharam FM, Ahmad K, Mansor S, Abu Seman I (2017a) Early detection of Ganoderma basal stem rot of oil palms using artificial neural network spectral analysis. Plant Dis 101(6):1009–1016. https://doi.org/10.1094/PDIS-12-16-1699-RE

Ahmadi P, Muharam FM, Ahmad K, Mansor S, Seman IA (2017b) Early detection of Ganoderma basal stem rot of oil palms using artificial neural network spectral analysis. Plant Dis 101(6):1009–1016

Chiang H-C, Wang Y, Zhang Q, Levon K (2019) Optimization of the electrodeposition of gold nanoparticles for the application of highly sensitive, label-free biosensor. Biosensors 9(2):50. https://doi.org/10.3390/bios9020050

Cho S, Chang T, Tianhao Yu, Lee CH (2022) Smart electronic textiles for wearable sensing and display. Biosensors 12(4):222. https://doi.org/10.3390/bios12040222

Choi YY, Kwon A, Majima Y (2019) Heteroepitaxial spherical electroless Au-plated Pt-based nanogap electrodes of radius 5 nm and gap separation 0.7 nm. Appl Phys Express 12(12):1–5. https://doi.org/10.7567/1882-0786/ab51df

Hamdy ME, Del Carlo M, Hussein HA, Salah TA, El-Deeb AH, Emara MM, Pezzoni G, Compagnone D (2018) Development of gold nanoparticles biosensor for ultrasensitive diagnosis of foot and mouth disease virus. J Nanobiotechnol 16:48. https://doi.org/10.1186/s12951-018-0374-x

Husin NA, Khairunniza-Bejo S, Abdullah AF, Kassim MS, Ahmad D, Azmi AN (2020) Application of ground-based LiDAR for analysing oil palm canopy properties on the occurrence of basal stem rot (BSR) disease. Sci Rep 10:1–16

Jiang P, Wang Y, Zhao L, Ji C, Chen D, Nie L (2018) Applications of gold nanoparticles in non-optical biosensors. Nanomaterials (basel) 8(12):977. https://doi.org/10.3390/nano8120977

Kang H, Jeong S, Yang J-K, Jo A, Lee H, Heo EH, Jeong DH, Jun B-H, Chang H, Lee Y-S (2021) Template-assisted plasmonic nanogap shells for highly enhanced detection of cancer biomarkers. Int J Mol Sci 22(4):1–13

Khaliq N, Rasheed MA, Khan M, Maqbool M, Ahmad M, Karim S, Nisar A, Schmuki P, Cho SO, Ali G (2021) ACS Appl Mater Interfaces 13(3):3653–3668. https://doi.org/10.1021/acsami.0c19979

Kumawat RL, Pathak B (2019) Individual Identification of DNA nucleobases on atomically thin black phosphorene nanoribbons: van der Waals corrected density functional theory calculations. J Phys Chem C 123(36):22377–22383

Kumawat RL, Pathak B (2021) Electronic conductance and current modulation through Graphdiyne nanopores for DNA sequencing. ACS Appl Electron Mater 3(9):3835–3845

Kumawat RL, Garg P, Kumar S, Pathak B (2019) Electronic transport through DNA nucleotides in atomically thin phosphorene electrodes for rapid DNA sequencing. ACS Appl Mater Interfaces 11(1):219–225

Lim T, Won S, Nam I-W, Choi JS, Kim CH, Kim TH, Kim JH, Yeo SY, Zhang H, Yeang BJ (2022) ACS Sustain Chem Eng 10(27):8815–8824. https://doi.org/10.1021/acssuschemeng.2c01556

Liu J, Liu J, Yang L, Chen X, Zhang M, Meng F, Luo T, Li M (2020) Nanomaterial-assisted signal enhancement of hybridization for DNA biosensors: a review. Sensors 9(9):7343–7364

Luo S, Mancini A, Berté R, Hoff BH, Maier SA, de Mello J (2020) Fabrication of size-controlled metallic nanogaps down to the sub 3-nm level. Cambridge Open Engage, Cambridge. ChemRxiv. (**This content is a preprint and has not been peer-reviewed**)

Namhil G, Kemp Z, Verrelli C, Iles E, Pamme A, Adawi N, Kemp AM, Neil TA (2020) label-free aptamer-based nanogap capacitive biosensor with greatly diminished electrode polarization effects. Phys Chem Chem Phys 21:681–691

Noor Azmi ANN, Bejo SK, Jahari M, Muharam FM, Yule I, Husin NA (2020a) Early detection of *Ganoderma boninense* in oil palm seedlings using support vector machines. Remote Sens 12(23):3920. https://doi.org/10.3390/rs12233920

Noor zmi AN, Bejo SK, Jahari M, Muharam FM, Yule I, Husin NA (2020b) Early detection of *Ganoderma boninense* in oil palm seedlings using support vector machines. Remote Sens 3920:1–21

Oh S-H, Altug H, Jin X, Low T, Koester S, Ivanov AP, Edel JB, Avouris P, Strano MS (2012) Nanophotonic biosensors harnessing van der Waals materials. Nat Commun 12:1–18. https://doi.org/10.2147/IJN.S181732

Pantazi XE, Tamouridou AA, Alexandridis TK, Lagopodi AL, Kontouris G, Moshou D (2017) Detection of *Silybum marianum* infection with *Microbotryum silybum* using VNIR field spectroscopy. Comput Electron Agric 137:130–137

Perez A, Amorim RG, Villegas CEP, Rocha AR (2020) Nanogap-based all-electronic DNA sequencing devices using MoS 2 monolayers. Phys Chem Chem Phys 22(46):27053–27059

Salazar A, Hosseini S, Sanchez-Domínguez M, Madou MJ, Montesinos-Castellanos A, Martinez-Chapa SO (2020) Sub-10 nm nanogap fabrication on suspended glassy carbon nanofibers. Microsyst Nanoeng 6(9):1–10

Shawky SM, Awad AM, Abugable AA, El-Khamisy SF (2018) Gold nanoparticles—an optical biosensor for RNA quantification for cancer and neurologic disorders diagnosis. Int J Nanomedicine 13:8137–8151. https://doi.org/10.2147/IJN.S181732

Shukla V, Jena NK, Grigoriev A, Ahuja R (2017) Prospects of graphene–hBN heterostructure nanogap for DNA sequencingy. ACS Appl Mater Interfaces 9(46):39945–39952

Siddiqui Y, ArthySurendran R, Paterson RM, Ali A, Ahmad K (2021) Current strategies and perspectives in detection and control of basal stem rot of oil palm. Saudi J Biol Sci 28(5):2840–2849. https://doi.org/10.1016/j.sjbs.2021.02.016

Tamari F, Hinkley CS, Ramprashad N (2013) A comparison of DNA extraction methods using *Petunia hybrida* tissues. J Biomol Tech 24(3):113–118. https://doi.org/10.7171/jbt.13-2403-001

Uda MNA, Gopinath SCB, Hashim U, Halim NH, Parmin NA, Uda MNA, Adam T, Anbu P (2021) Silica and graphene mediate arsenic detection in mature rice grain by a newly patterned current-volt aptasensor. Sci Rep 11(1):14688–14695

Zhao Z-J, Ahn J, Hwang SH, Ko J, Jeong Y, Bok M, Kang H-J, Choi J, Jeon S, Park I, Jeong J-H (2021) Large-area nanogap-controlled 3D nanoarchitectures fabricated via layer-by-layer nanoimprint. ACS Nano 15(1):503–514